


Article

# Soft X-ray Absorption Spectroscopy Study of Spin Crossover Fe-Compounds: Persistent High Spin Configurations under Soft X-ray Irradiation

Ahmed Yousef Mohamed <sup>1,2</sup>, Minji Lee <sup>1</sup>, Kosuke Kitase <sup>3</sup>, Takafumi Kitazawa <sup>3,4</sup> ,  
Jae-Young Kim <sup>5</sup> and Deok-Yong Cho <sup>1,\*</sup>

<sup>1</sup> IPIT & Department of Physics, Chonbuk National University, Jeonju 54896, Korea; yousef@jbnu.ac.kr (A.Y.M.); mj9834@jbnu.ac.kr (M.L.)

<sup>2</sup> Department of Physics, South Valley University, Qena 83523, Egypt

<sup>3</sup> Department of Chemistry, Toho University, Chiba 274-8510, Japan; 6117004k@st.toho-u.ac.jp (K.K.); kitazawa@chem.sci.toho-u.ac.jp (T.K.)

<sup>4</sup> Research Centre for Materials with Integrated Properties, Toho University, Chiba 274-8510, Japan

<sup>5</sup> Center for Artificial Low Dimensional Electronic Systems, Institute for Basic Science (IBS), Pohang 37673, Korea; jaeyoung@ibs.re.kr

\* Correspondence: zax@jbnu.ac.kr; Tel.: +82-63-270-3444

Received: 19 October 2018; Accepted: 16 November 2018; Published: 19 November 2018



**Abstract:** Metal-organic complex exhibiting spin crossover (SCO) behavior has drawn attention for its functionality as a nanoscale spin switch. The spin states in the metal ions can be tuned by external stimuli such as temperature or light. This article demonstrates a soft X-ray-induced excited spin state trapping (SOXEISST) effect in Hofmann-like SCO coordination polymers of  $\text{Fe}^{\text{II}}(4\text{-methylpyrimidine})_2[\text{Au}(\text{CN})_2]_2$  and  $\text{Fe}^{\text{II}}(\text{pyridine})_2[\text{Ni}(\text{CN})_4]$ . A soft X-ray absorption spectroscopy (XAS) study on these polymers showed that the high spin configuration (HS;  $S = 2$ ) was prevalent in  $\text{Fe}^{2+}$  ions during the measurement even at temperatures much lower than the critical temperatures ( $>170$  K), manifesting HS trapping due to the X-ray irradiation. This is in strong contrast to the normal SCO behavior observed in  $\text{Fe}^{\text{II}}(1,10\text{-phenanthroline})_2(\text{NCS})_2$ , implying that the structure of the ligand chains in the polymers with relatively loose Fe-N coordination might allow a structural adaptation to stabilize the metastable HS state under the soft X-ray irradiation.

**Keywords:** spin crossover; X-ray absorption spectroscopy; soft X-ray induced excited spin state trapping; high spin

## 1. Introduction

Since the first report on spin-crossover (SCO) molecules from Cambi and Szegö in 1931 [1], metal-organic complexes have been the subjects of many studies [2–5] due to the possibility of their use as nanoscale molecular spin switches [6–10]. The SCO phenomenon which involves a change in the spin state of the metal ion, can be caused by many kinds of external stimuli including variation of temperature [11,12] or pressure [13], or the influence of ligand chemistry [14], light or X-ray irradiation [15–22] or electromagnetic field [23,24]. When the structures of the molecular networks change in a cooperative manner associated with the spin crossover, the transition occurs with steepness and/or sometimes is accompanied by a hysteresis loop (the first order transition). Thus, the SCO molecular materials can offer many possible applications in the fields of electronics, information storage, digital display, photonics or photo-magnetism, etc.

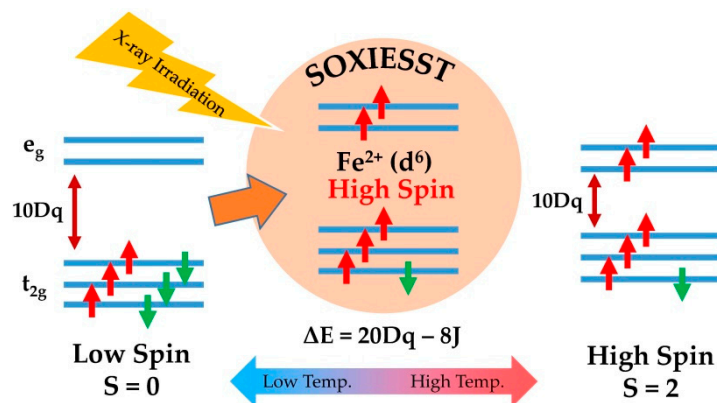
In most cases of the SCO metal complexes reported so far, the change in the spin state occurs from a low spin (LS) ground state configuration to a high spin (HS) metastable configuration of the metal ion's  $d$  electrons. At low temperatures below a transition temperature,  $T_C$ , the LS configuration is prevalent, while at temperatures higher than  $T_C$ , HS configuration becomes dominant. The population ratio between the LS and HS configurations at a given temperature, is determined by the competition of the Hund coupling in the  $d$  shell with the strength of the ligand fields from the nearest atoms. According to the ligand field theory, the splitting of the  $d$  orbital energies is determined by the coordination symmetry and bond lengths of the metal ions.

Figure 1 illustrates the metal's  $d$  orbital exemplary splitting under octahedral ligand field for  $\text{Fe}^{2+}$  ( $d^6$ ) ions. The  $d$  orbital energy splits into a triplet  $t_{2g}$  level at a lower energy and a doublet  $e_g$  level at a higher energy under the octahedral ligand field, and six electrons fill the levels. When all the electrons occupy the  $t_{2g}$  levels only following the order of the ligand field splitting energy, the value of the total spin ( $S$ ) should be zero, and thereby, the electron configuration is called LS [25]. Meanwhile, when two of the electrons occupy  $e_g$  levels following the preference of the spin alignment (Hund's coupling), the value of  $S$  should be maximized ( $S = 2$ ); thus, the configuration is called HS. To attain a HS configuration, each of the two electrons should overcome the ligand field splitting energies ( $10 Dq$ ), but at the same time, obtain the energies of Hund exchanges with the other four electrons ( $-4 J$ ), so that the energy difference between the HS and LS should be  $\Delta E = 20 Dq - 8 J$ . It has been shown that the ligand field strength ( $10 Dq$ ) can significantly influence the population ratio [26,27]. Generally, as bond lengths of the metal ions to the ligands are longer, the HS configuration can be favored more because of the lower  $10 Dq$ . Since the bond lengths tend to increase with increasing temperature, HS can be stabilized more at higher temperatures.

The SCO phenomena can be explored by various magnetic and spectroscopic techniques including magnetic susceptibility measurement, Mössbauer spectroscopy [28,29], optical absorption and X-ray absorption spectroscopy (XAS) [4,30,31]. In those experimental techniques, external stimuli are applied to the specimen in order to observe the responses related to the spin states. For instance, XAS at Fe  $L_{2,3}$ -edge utilizes the electronic excitation from the  $2p$  core level to the  $3d$  unoccupied state following the X-ray perturbation. Previous Fe  $L_{2,3}$ -edge XAS studies on a representative SCO molecule,  $\text{Fe}(\text{phen})_2(\text{NCS})_2$  at low and high temperatures, have established a set of spectroscopic fingerprints for the HS and LS states [32–35].

However, one cannot exclude a possibility that the stimulus itself can change the properties of the specimen. Indeed, in the case of soft XAS, it has been reported that the spin state can change under the X-ray irradiation during the measurement. Such soft X-ray-induced excited spin state trapping (SOXIESST) effects can lead to persistent HS configuration even below  $T_C$  [21,22]. The SOXIESST effect has been regarded as a result of temporary trapping in the HS due to the cascade of excitations by illumination, similar to the case of light-induced excited spin state trapping (LIESST) [26,27]. For instance, the SOXIESST effect was described in detail on  $\text{Fe}(\text{phen})_2(\text{NCS})_2$  and  $\text{Fe}[\text{Me}_2\text{Pyrz}]_3\text{BH}_2$  by V. Davesne et al. [21,36].

Earlier studies have suggested that the mechanism of the SOXIESST effect is analogous to that of the LIESST effect [19,21,22,35]; their similarities and differences were discussed by V. Davesne et al. [21,27,36]. Namely, the light or X-ray introduction leads to an excitation of the system from the LS ground state configuration to the excited state configurations and it follows that the excited state configurations decay into a metastable spin triplet HS configuration (intersystem crossing). Then the spin states can remain trapped in this excited HS state, unless the temperature is high enough to overcome the energy barrier between the HS and LS configurations via the thermal fluctuations [19,21,22,35]. However, when X-rays are turned off, the system again favors the LS ground state configuration. In this regard, SOXIESST is a reversible process. Meanwhile, the soft X-ray photochemistry (SOXPC) effect can alter the chemistry of specimens in an irreversible way. D. Collison et al. [22] showed that although the (reversible) SOXIESST effect is predominant in  $\text{Fe}(\text{phen})_2(\text{NCS})_2$ , the (irreversible) SOXPC effect also exists and plays in a competitive manner.



**Figure 1.** Illustration of the  $\text{Fe}^{2+}$  ( $d^6$ )  $d$  orbital energy splitting under octahedral ligand field and the resultant LS (low spin) and HS (high spin) configurations. The SCO (spin crossover) from LS to HS with increasing temperature can be explained by the weakened ligand field, i.e., lower  $10 Dq$ . If a soft X-ray-induced excited spin state trapping (SOXIESST) effect is activated, HS configuration is persistent even at temperatures below  $T_C$ .

This article reports a SOXIESST effect in Hofmann-like SCO coordination polymers,  $\text{Fe}(\text{4-methylpyrimidine})_2[\text{Au}(\text{CN})_2]_2$  ( $\text{Fe}(\text{4-methylpmd})_2[\text{Au}(\text{CN})_2]_2$ ) and  $\text{Fe}(\text{pyridine})_2[\text{Ni}(\text{CN})_4]$  ( $\text{Fe}(\text{py})_2[\text{Ni}(\text{CN})_4]$ ). Figure 2 illustrates the molecular structures of the two polymers in comparison to a well-known SCO complex,  $\text{Fe}(\text{1,10-phenanthroline})_2(\text{NCS})_2$  ( $\text{Fe}(\text{phen})_2(\text{NCS})_2$ ). Compared to the latter, the two polymers (Figure 2a) have relatively loose Fe-N coordinations, in that all the N ions in the ligands are in separate chains, while many of the N ions in  $\text{Fe}(\text{phen})_2(\text{NCS})_2$  are bound to benzene-like rings (Figure 2b). The less rigid Fe-N coordination could somehow offer a ground for spin state transition upon external stimuli such as X-ray irradiation. Therefore, soft XAS was performed to examine the possible SOXIESST effects in the loosely coordinated  $\text{Fe}^{2+}$  ions in the polymeric structures.

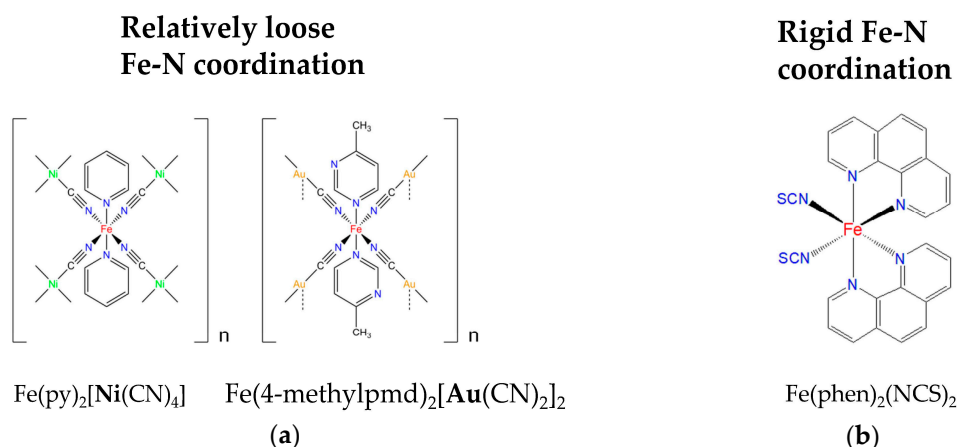


**Figure 2.** Molecular structures of (a) Hofmann-like SCO polymers of  $\text{Fe}(\text{4-methylpmd})_2[\text{Au}(\text{CN})_2]_2$  and  $\text{Fe}(\text{py})_2[\text{Ni}(\text{CN})_4]$ , and (b) a reference  $\text{Fe}(\text{phen})_2(\text{NCS})_2$ .

## 2. Materials and Methods

$\text{Fe}(\text{4-methylpmd})_2[\text{Au}(\text{CN})_2]_2$ ,  $\text{Fe}(\text{py})_2[\text{Ni}(\text{CN})_4]$  and  $\text{Fe}(\text{phen})_2(\text{NCS})_2$  powders were synthesized by the vapor diffusion methods. Details on the preparation for  $\text{Fe}(\text{py})_2[\text{Ni}(\text{CN})_4]$  and  $\text{Fe}(\text{phen})_2(\text{NCS})_2$  were the same as reported in References [8,37].  $\text{Fe}(\text{4-methylpmd})_2[\text{Au}(\text{CN})_2]_2$  was prepared by the same method for the synthesis of  $\text{Fe}(\text{4-methylpy})_2[\text{Au}(\text{CN})_2]_2$  [9].

The compositions and structures of the three powder samples were identified by elemental analysis, powder X-ray diffraction (XRD), and infrared (IR) spectroscopy. The elemental analysis for C, H and N was carried out with CHN CORDER JM10 (Yanaco Corp., Tokyo, Japan). The results

of the elemental analysis suggest a Hofmann-type-like formula of  $\text{Fe}(4\text{-methylpmd})_2[\text{Au}(\text{CN})_2]_2$  (Found: C, 22.57%; H, 1.75%; N, 15.07%; Calculated: C, 22.66%; H, 1.68%; N, 15.10%), the Hofmann-type formula of  $\text{Fe}(\text{py})_2[\text{Ni}(\text{CN})_4]$  [8] (Found: C, 44.40%; H, 1.75%; N, 22.02%; Calculated: C, 44.62%; H, 1.68%; N, 22.31%), and the mononuclear complex formula of  $\text{Fe}(\text{phen})_2(\text{NCS})_2$  [37] (Found: C, 58.44%; H, 3.32%; N, 15.63%; Calc. C, 58.65%; H, 3.03%; N, 15.791%).

IR spectra were obtained by the Nujol mull method using JASCO FTIR-4100 spectrometer (JASCO Corp., Hachioji, Japan). The spectra for the three samples are shown in Figure S1 in the Supplementary Information (SI). For  $\text{Fe}(4\text{-methylpmd})_2[\text{Au}(\text{CN})_2]_2$ , wavenumbers of the dips,  $\nu_{\text{max}}$ 's were 2170, 1619, 1599, 1556, 1492, 1325, 1014 and 845 in  $\text{cm}^{-1}$  (Figure S1a). The CN stretching band at  $2170 \text{ cm}^{-1}$  originates from the linkage between  $\text{Au}^+$  and  $\text{Fe}^{2+}$  ions. For  $\text{Fe}(\text{py})_2[\text{Ni}(\text{CN})_4]$ ,  $\nu_{\text{max}}$ 's were 2158, 1603, 1573, 1218, 1152, 1038, 1011, 751, 690, 626, 437 and 419 in  $\text{cm}^{-1}$  (Figure S1b). The CN stretching band ( $2158 \text{ cm}^{-1}$ ) is due to linkage between  $\text{Ni}^{2+}$  and  $\text{Fe}^{2+}$  ions. For  $\text{Fe}(\text{phen})_2(\text{NCS})_2$ ,  $\nu_{\text{max}}$ 's were 2072 and 2060 in  $\text{cm}^{-1}$  (Figure S1c).

Powder XRD pattern of  $\text{Fe}(4\text{-methylpmd})_2[\text{Au}(\text{CN})_2]_2$  was obtained by using a Rigaku RINT2500 diffractometer (Rigaku Corp., Akishima, Japan) with graphite-monochromated  $\text{Cu K}\alpha$  radiation ( $\lambda = 1.5406 \text{ \AA}$ ). Figure S2 in SI shows the XRD pattern. It is similar to that from  $\text{Fe}(4\text{-methylpy})_2[\text{Au}(\text{CN})_2]_2$  [9].

Thermal decomposition of  $\text{Fe}(4\text{-methylpmd})_2[\text{Au}(\text{CN})_2]_2$  was investigated on TG/DTA6200 (SII Nano Technology, Chiba, Japan) under a dry  $\text{N}_2$  gas flow by recording the thermogravimetric (TG) curve. Figure S3 in SI shows the TG curve. The 25.4% weight loss at the plateau between 577 K and 617 K corresponds to the thermal decomposition of  $\text{Fe}(4\text{-methylpmd})_2[\text{Au}(\text{CN})_2]_2$  into  $\text{Fe}[\text{Au}(\text{CN})_2]_2$ .

Magnetic susceptibility was measured in the temperature range of 4–300 K with a cooling and heating rate of 2 K/min in a 0.1 Tesla field using a MPMS-XL Quantum Design SQUID magnetometer.

For the XAS, the three powder samples were attached gently on carbon tapes. Fe  $L_{2,3}$ -edge XAS was performed at 2 A beamline in Pohang Light Source. Absorption coefficients were collected with increasing photon energy in total electron yield mode at various temperatures. The intensity of the incident X-rays was estimated to be approximately  $3 \times 10^{11}$  photons/s/mm<sup>2</sup>. The beam flux was sufficiently low so that a SOXIESST did not occur in the reference  $\text{Fe}(\text{phen})_2(\text{NCS})_2$  powder as is evident in the XAS spectra. The samples were not intentionally exposed to X-rays before the measurement, and the measurement time for each data was approximately 10 min.

### 3. Results and Discussion

#### 3.1. Magnetic Susceptibility

Figure 3 shows the magnetic susceptibility of the specimens. Theoretically, magnetic susceptibility ( $\chi_m$ ) of a paramagnet is proportional to  $J(J + 1)/T$ , where  $J$  is the total angular momentum quantum number and  $T$  is the temperature. All the data from the specimens show clear step-like jumps of  $\chi_m T$  with increasing temperature at  $T_C$ 's ranging from 175 K to 205 K [38,39], suggesting an increase of the  $J$  value at high temperature. Generally, such an increase is caused by the increase in the spin angular momentum, while the angular momentum in the metal ion under the octahedral coordination is generally much smaller than the nominal value (two for  $d$ -orbitals) due to the orbital momentum quenching effect. Therefore, we can tell that for instance, at  $T = 110$  K, the three powder samples were all in the LS ( $S = 0$ ) state, while at room temperature, those were all in the HS ( $S = 2$ ) state. Thus, it is clearly shown in the magnetization data that all the samples show strong SCO behaviors (when no soft X-ray beams were applied). It might be interesting to note that in the case of  $\text{Fe}(4\text{-methylpy})_2[\text{Au}(\text{CN})_2]_2$ , two steps were observed without a hysteresis, similar to the case of  $\text{Fe}(3\text{-F-4-methylpy})_2[\text{Au}(\text{CN})_2]_2$  [10]. Details in the multistep SCO will be discussed elsewhere. The irregular noises in the data of  $\text{Fe}(\text{phen})_2(\text{NCS})_2$  at temperatures below 170 K, presumably originate from nonuniform sample packing due to a relatively small amount of the specimen.

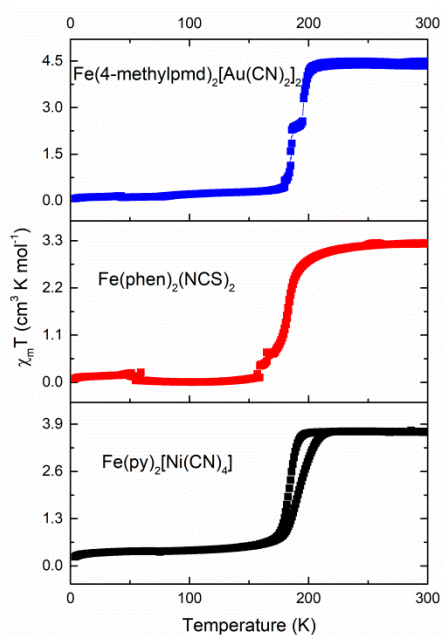


**Figure 3.** Magnetic susceptibility multiplied by temperature ( $\chi_m T$ ) showing the LS-to-HS SCO with increasing temperature across  $T_C$ 's ranging from 175 K to 205 K.

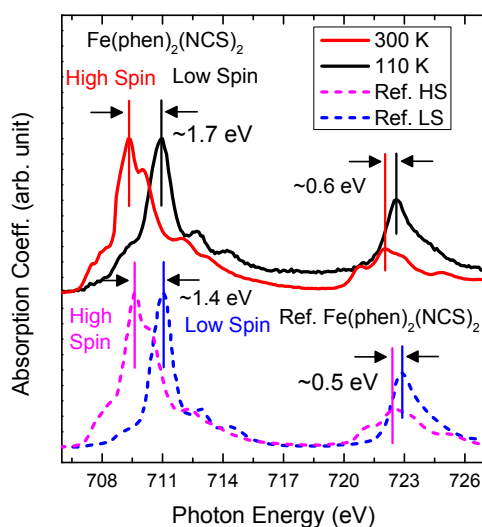
### 3.2. Soft X-ray Absorption Spectroscopy

Figure 4 shows the Fe  $L_{2,3}$ -edge XAS spectra of  $\text{Fe}(\text{phen})_2(\text{NCS})_2$  complex recorded at 300 and 110 K. The spectra show that the peak positions and the lineshapes evolved with temperature remarkably. Compared to the spectrum taken at 300 K, the spectrum taken at 110 K shifted to higher energies overall; 1.7 eV for the  $L_3$  (features around 710 eV) and 0.6 eV for the  $L_2$ -edge maxima (features around 723 eV). Also, the  $L_2$ -edge features become consolidated at the lower temperature.

For comparison, the spectra for the same composition from a literature [34] are appended as the dotted curves in the figure. Each of the spectra (taken at 300 K and 110 K) resemble the respectively dotted curves. In many literatures, the lineshapes of the spectra have been interpreted as the fingerprints of the HS  $\text{Fe}^{2+}$  (for 300 K) and LS  $\text{Fe}^{2+}$  (for 110 K) under octahedral ligand fields [22,24,32,34,40]. The clear spectral evolution upon the temperature increase suggests that a certain SOXIESST effect has not occurred in the  $\text{Fe}(\text{phen})_2(\text{NCS})_2$  complex. Therefore, we can conclude that the intensity of the soft X-rays ( $\sim 3 \times 10^{11}$  photons/sec/mm<sup>2</sup>) was not high enough to evoke a SOXIESST effect in the reference  $\text{Fe}(\text{phen})_2(\text{NCS})_2$  powder. Compared to the case of thin film samples [32–35], the powder specimen appears more resistant to the SOXIESST effect upon X-ray exposure. Probably, this is because the powders are distributed sparsely so that the actual intensity of the beam shed on the SCO complex should be much weaker than the nominal value. As can be seen in Figure 2, the Fe-N coordination in  $\text{Fe}(\text{phen})_2(\text{NCS})_2$  complex is rigid, being surrounded by benzene-like rings, so the Fe-N bond lengths, which are closely related to the preference of HS/LS population, would hardly change under the external stimuli like X-ray irradiation with a low flux.

On the other hand, the spectra of the two polymers clearly shows the SOXIESST effect. Figure 5 shows the Fe  $L_{2,3}$ -edge XAS spectra of the  $\text{Fe}^{\text{II}}$  complexes with polymeric structures. For both compositions of (a)  $\text{Fe}(\text{4-methylpmd})_2[\text{Au}(\text{CN})_2]_2$  and (b)  $\text{Fe}(\text{py})_2[\text{Ni}(\text{CN})_4]$ , the lineshapes and the peak positions in the spectra were mostly similar to that of a HS  $\text{Fe}^{2+}$ , manifesting a prevalence of HS even at 110 K, far below the  $T_C$ 's ( $>170$  K). Note that, however, the persistent HS is not consistent with the observation in the magnetic susceptibility measurement (Figure 3), which showed clear LS-to-HS SCO behaviors for all the samples. Then the persistent HS observed in soft XAS can be understood only by considering certain excitation effects of the soft X-ray introduction;

under the X-ray irradiation, the system might be excited to possess a metastable HS configuration even at low temperatures.



**Figure 4.** Fe  $L_{2,3}$ -edge XAS spectra of  $\text{Fe}(\text{phen})_2(\text{NCS})_2$  complex recorded at 300 K (above  $T_C$ ) and 110 K (below  $T_C$ ), with reference spectra from the same composition [34], clearly showing a LS-HS SCO without any SOXIESST effect.

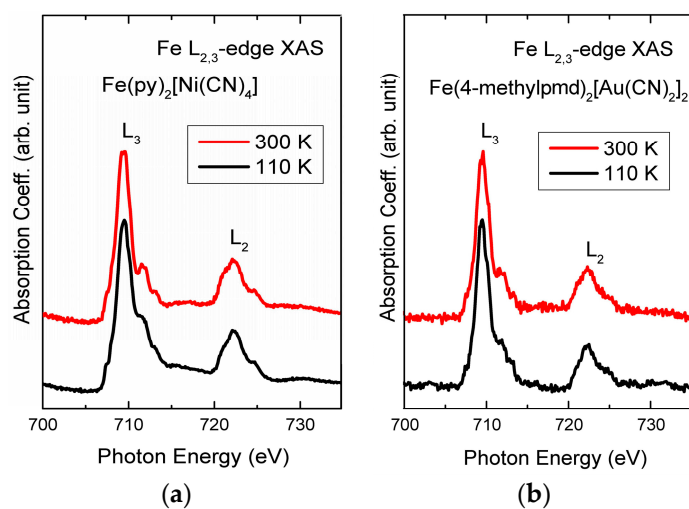


**Figure 5.** Fe  $L_{2,3}$ -edge XAS spectra of (a)  $\text{Fe}(4\text{-methylpmd})_2[\text{Au}(\text{CN})_2]_2$  and (b)  $\text{Fe}(\text{py})_2[\text{Ni}(\text{CN})_4]$  polymers. HS configuration was dominant even at 110 K (below  $T_C$ ), suggesting SOXIESST effects for the loosely coordinated polymers.

This is in clear contrast to the case of reference,  $\text{Fe}(\text{phen})_2(\text{NCS})_2$  (Figure 4), which showed no SOXIESST effect. Although the three spectra were taken with the same beam flux, the two polymer samples appear to possess HS state while  $\text{Fe}(\text{phen})_2(\text{NCS})_2$  was relatively resistant to the weak X-rays. The distinction might originate from the different structures of the bonds. Since the bond chains in the two polymers are formed only in radial directions with respect to the  $\text{Fe}^{2+}$  ions at the center (see Figure 2a), the Fe-N coordination would be relatively free to rotate or to be elongated. Such structural freedom in the coordination polymers can somehow act to facilitate the stabilization of the metastable HS state.

#### 4. Conclusions

In conclusion, results of soft XAS on Hofmann-like  $\text{Fe}^{\text{II}}(4\text{-methylpyrimidine})_2[\text{Au}(\text{CN})_2]_2$  and  $\text{Fe}^{\text{II}}(\text{pyridine})_2[\text{Ni}(\text{CN})_4]$  polymers showed that the high spin configuration prevailed even at temperatures far below the  $T_C$ 's (despite the normal SCO behaviors in magnetic susceptibility), suggesting that the SOXIESST effects were activated to suppress the SCO effects. This was in contrast to the reference  $\text{Fe}(\text{phen})_2(\text{NCS})_2$  complex, in which a clear SCO was observed by soft XAS; thereby, we suspect that the relatively loose Fe-N coordination in the Hofmann-like coordination polymers might be responsible for the SOXIESST effects.

**Supplementary Materials:** The following are available online at <http://www.mdpi.com/2073-4352/8/11/433/s1>, Figure S1: FT-IR spectroscopy analysis of (a)  $\text{Fe}(4\text{-methylpmd})_2[\text{Au}(\text{CN})_2]_2$ , (b)  $\text{Fe}(\text{py})_2[\text{Ni}(\text{CN})_4]$ , and (c)  $\text{Fe}(\text{phen})_2(\text{NCS})_2$ , Figure S2: Powder XRD pattern of  $\text{Fe}(4\text{-methylpmd})_2[\text{Au}(\text{CN})_2]_2$ , Figure S3: Thermogravimetric analysis (TGA) of  $\text{Fe}(4\text{-methylpmd})_2[\text{Au}(\text{CN})_2]_2$ .

**Author Contributions:** Conceptualization, T.K. and D.-Y.C.; Soft XAS, A.Y.M., M.L., J.-Y.K. and D.-Y.C.; Samples, Magnetization and preliminary measurements, K.K. and T.K.

**Funding:** This research was funded by National Research Foundation of Korea, grant number NRF-2018R1D1A1B07043427 and Japan Society for the Promotion Science (JSPS) KAKENHI Grant Number 15K05485.

**Acknowledgments:** The authors thank Daisuke Akahoshi and Toshiaki Saito in Department of Physics, Toho University for the SQUID measurements.

**Conflicts of Interest:** The authors declare no conflict of interest. The funders had no role in the design of the study; in the collection, analyses, or interpretation of data; in the writing of the manuscript, or in the decision to publish the results.

#### References

1. Cambi, L.; Szegzi, L. Über die magnetische Suszeptibilität der komplexen Verbindungen. *Berichte Dtsch. Chem. Gesellschaft B* **1931**, *64*, 2591–2598. [[CrossRef](#)]
2. Gütlich, P.; Goodwin, H.A. *Spin Crossover in Transition Metal I*; Gütlich, P., Goodwin, H.A., Eds.; Springer: Berlin/Heidelberg, Germany, 2004. [[CrossRef](#)]
3. Gütlich, P.; Garcia, Y.; Goodwin, H.A. Spin crossover phenomena in Fe(ii) complexes. *Chem. Soc. Rev.* **2000**, *29*, 419–427. [[CrossRef](#)]
4. Real, J.A.; Gaspar, A.B.; Munoz, M.C. Thermal, pressure and light switchable spin-crossover materials. *Dalton. Trans.* **2005**, 2062–2079. [[CrossRef](#)] [[PubMed](#)]
5. Murray, K.S. *Spin-Crossover Materials*; Halcrow, M.A., Ed.; John Wiley & Sons, Ltd.: London, UK, 2013.
6. Létard, J.-F.; Guionneau, P.; Goux-Capes, L. Towards Spin Crossover Applications. *Top. Curr. Chem.* **2004**, *235*, 221–249. [[CrossRef](#)]
7. Marchivie, M.; Guionneau, P.; Howard, J.A.K.; Chastanet, G.; Létard, J.-F.; Goeta, A.E.; Chasseau, D. Structural Characterization of a Photoinduced Molecular Switch. *J. Am. Chem. Soc.* **2002**, *124*, 194–195. [[CrossRef](#)] [[PubMed](#)]
8. Kitazawa, T.; Gomi, Y.; Takahashi, M.; Takeda, M.; Enomoto, M.; Miyazaki, A.; Enoki, T. Spin-crossover behaviour of the coordination polymer  $\text{Fe}^{\text{II}}(\text{C}_5\text{H}_5\text{N})_2\text{Ni}^{\text{II}}(\text{CN})_4$ . *J. Mater. Chem.* **1996**, *6*, 119–121. [[CrossRef](#)]
9. Kosone, T.; Tomori, I.; Kanadani, C.; Saito, T.; Mochida, T.; Kitazawa, T. Unprecedented three-step spin-crossover transition in new 2-dimensional coordination polymer  $\{\text{Fe}^{\text{II}}(4\text{-methylpyridine})_2[\text{Au}^{\text{I}}(\text{CN})_2]_2\}$ . *Dalton Trans.* **2010**, 39, 1719–1721. [[CrossRef](#)] [[PubMed](#)]
10. Kosone, T.; Kawasaki, T.; Tomori, I.; Okabayashi, J.; Kitazawa, T. Modification of Cooperativity and Critical Temperatures on a Hofmann-Like Template Structure by Modular Substituent. *Inorganics* **2017**, *5*, 55. [[CrossRef](#)]
11. Wu, Z.; Justo, J.F.; da Silva, C.R.S.; de Gironcoli, S.; Wentzcovitch, R.M. Anomalous thermodynamic properties in ferropentacycline throughout its spin crossover. *Phys. Rev. B* **2009**, *80*. [[CrossRef](#)]
12. Wentzcovitch, R.M.; Justo, J.F.; Wu, Z.; da Silva, C.R.; Yuen, D.A.; Kohlstedt, D. Anomalous compressibility of ferropentacycline throughout the iron spin cross-over. *Proc. Natl. Acad. Sci. USA* **2009**, *106*, 8447–8452. [[CrossRef](#)] [[PubMed](#)]

13. Ksenofontov, V.; Gaspar, A.B.; Gütllich, P. Pressure Effect Studies on Spin Crossover and Valence Tautomeric Systems. In *Spin Crossover in Transition Metal III*; Gütllich, P., Goodwin, H.A., Eds.; Springer: Berlin/Heidelberg, Germany, 2004. [[CrossRef](#)]
14. Boillot, M.-L.; Zarembowitch, J.; Sour, A. Ligand-Driven Light-Induced Spin Change (LD-LISC): A Promising Photomagnetic Effect. In *Spin Crossover in Transition Metal II*; Gütllich, P., Goodwin, H.A., Eds.; Springer: Berlin/Heidelberg, Germany, 2004. [[CrossRef](#)]
15. Naggert, H.; Bannwarth, A.; Chemnitz, S.; von Hofe, T.; Quandt, E.; Tuzek, F. First observation of light-induced spin change in vacuum deposited thin films of iron spin crossover complexes. *Dalton Trans.* **2011**, *40*, 6364–6366. [[CrossRef](#)] [[PubMed](#)]
16. Cannizzo, A.; Milne, C.J.; Consani, C.; Gawelda, W.; Bressler, C.; van Mourik, F.; Chergui, M. Light-induced spin crossover in Fe(II)-based complexes: The full photocycle unraveled by ultrafast optical and X-ray spectroscopies. *Coord. Chem. Rev.* **2010**, *254*, 2677–2686. [[CrossRef](#)]
17. Herber, R.; Casson, L.M. Light-Induced Excited-Spin-State Trapping: Evidence from VTFTIR Measurements. *Inorg. Chem.* **1986**, *25*, 847–852. [[CrossRef](#)]
18. Hauser, A. Light-Induced Spin Crossover and the High-Spin → Low-Spin Relaxation. In *Spin Crossover in Transition Metal II*; Gütllich, P., Goodwin, H.A., Eds.; Springer: Berlin/Heidelberg, Germany, 2004. [[CrossRef](#)]
19. Decurtins, S.; Gütllich, P.; Hasselbach, K.M.; Hauser, A.; Spiering, H. Light-Induced Excited-Spin-State Trapping in Iron(II) Spin-Crossover Systems. Optical Spectroscopic and Magnetic Susceptibility Study. *Inorg. Chem.* **1985**, *24*, 2174–2178. [[CrossRef](#)]
20. Hauser, A. Reversibility of light-induced excited spin state trapping in the Fe(ptz)<sub>6</sub>(BF<sub>4</sub>)<sub>2</sub> and the Zn<sub>1-x</sub>Fe<sub>x</sub>(ptz)<sub>6</sub>(BF<sub>4</sub>)<sub>2</sub> spin-crossover systems. *Chem. Phys. Lett.* **1986**, *124*, 543–548. [[CrossRef](#)]
21. Davesne, V.; Gruber, M.; Miyamachi, T.; Da Costa, V.; Boukari, S.; Scheurer, F.; Joly, L.; Ohresser, P.; Otero, E.; Choueikani, F.; et al. First glimpse of the soft X-ray induced excited spin-state trapping effect dynamics on spin cross-over molecules. *J. Chem. Phys.* **2013**, *139*, 074708. [[CrossRef](#)] [[PubMed](#)]
22. Collison, D.; Garner, C.D.; McGrath, C.M.; Mosselmanns, J.F.W.; Roper, M.D.; Seddon, J.M.W.; Sinn, E.; Young, N.A. Soft X-ray induced excited spin state trapping and soft X-ray photochemistry at the iron L<sub>2,3</sub> edge in [Fe(phen)<sub>2</sub>(NCSe)<sub>2</sub>] and [Fe(phen)<sub>2</sub>(NCS)<sub>2</sub>] (phen = 1,10-phenanthroline). *J. Chem. Soc. Dalton Trans.* **1997**, *22*, 4371–4376. [[CrossRef](#)]
23. Bousseksou, A.; Varret, F.; Goiran, M.; Boukheddaden, K.; Tuchagues, J.P. The Spin Crossover Phenomenon Under High Magnetic Field. In *Spin Crossover in Transition Metal III*; Gütllich, P., Goodwin, H.A., Eds.; Springer: Berlin/Heidelberg, Germany, 2004. [[CrossRef](#)]
24. Miyamachi, T.; Gruber, M.; Davesne, V.; Bowen, M.; Boukari, S.; Joly, L.; Scheurer, F.; Rogez, G.; Yamada, T.K.; Ohresser, P.; et al. Robust spin crossover and memristance across a single molecule. *Nat. Commun.* **2012**, *3*, 938. [[CrossRef](#)] [[PubMed](#)]
25. Cotton, F.; Wilkinson, G.; Gaus, P. *Basic Inorganic Chemistry*, 3rd ed.; Cotton, F., Wilkinson, G., Gaus, P., Eds.; Wiley: New York, NY, USA, 1995. [[CrossRef](#)]
26. Wäckerlin, C.; Donati, F.; Singha, A.; Baltic, R.; Decurtins, S.; Liu, S.-X.; Rusponi, S.; Dreiser, J. Excited Spin-State Trapping in Spin Crossover Complexes on Ferroelectric Substrates. *J. Phys. Chem. C* **2018**, *122*, 8202–8208. [[CrossRef](#)]
27. Davesne, V. Organic Spintronics: An Investigation on Spin-Crossover Complexes from Isolated Molecules to the Device. Ph.D. Thesis, Physique et Chimie Physique Université de strasbourg, Strasbourg, France, 2013.
28. Kitazawa, T.; Kawasaki, T.; Shiina, H.; Takahashi, M. Mössbauer Spectroscopic Study on Hofmann-like Coordination Polymer Fe(4-Clpy)<sub>2</sub>[Ni(CN)<sub>4</sub>]. *Croat. Chem. Acta* **2016**, *89*, 111–115. [[CrossRef](#)]
29. Kitazawa, T.; Kishida, T.; Kawasaki, T.; Takahashi, M. Spin crossover behaviour in Hofmann-like coordination polymer Fe(py)<sub>2</sub>[Pd(CN)<sub>4</sub>] with 57Fe Mössbauer spectra. *Hyperfine Interact.* **2017**, *238*. [[CrossRef](#)]
30. Gütllich, P.; Goodwin, H.A. Spin Crossover—An Overall Perspective. *Top. Curr. Chem.* **2004**, *233*, 1–47. [[CrossRef](#)]
31. Ueki, Y.; Okabayashi, J.; Kitazawa, T. Guest Molecule Inserted Spin Crossover Complexes: Fe[4-(3-Pentyl)pyridine]<sub>2</sub>[Au(CN)<sub>2</sub>]<sub>2</sub>·Guest. *Chem. Lett.* **2017**, *46*, 747–749. [[CrossRef](#)]
32. Moulin, C.C.D.; Rudolf, P.; Flank, A.M.; Chen, C.T. Spin Transition Evidenced by Soft X-ray Absorption Spectroscopy. *J. Phys. Chem.* **1992**, *96*, 6196–6198. [[CrossRef](#)]



33. Moulin, C.C.D.; Flank, A.M.; Rudolf, P.; Chen, C.T. Electronic Structure from Iron L-edge Spectroscopy: An Example of Spin Transition Evidenced by Soft X-ray Absorption Spectroscopy. *Jpn. J. Appl. Phys.* **1993**, *32* (Suppl. 2), 308–310. [[CrossRef](#)]
34. Briois, V.; Moulin, C.C.D.; Saintavit, P.; Brouder, C.; Flank, A.-M. Full Multiple Scattering and Crystal Field Multiplet Calculations Performed on the Spin Transition  $\text{Fe}^{\text{II}}(\text{phen})_2(\text{NCS})_2$  Complex at the Iron K and  $L_{2,3}$  X-ray Absorption Edges. *J. Am. Chem. Soc.* **1995**, *117*, 1019–1026. [[CrossRef](#)]
35. Kipgen, L.; Bernien, M.; Ossinger, S.; Nickel, F.; Britton, A.J.; Arruda, L.M.; Naggert, H.; Luo, C.; Lotze, C.; Ryll, H.; et al. Evolution of cooperativity in the spin transition of an iron(II) complex on a graphite surface. *Nat. Commun.* **2018**, *9*, 2984. [[CrossRef](#)] [[PubMed](#)]
36. Davesne, V.; Gruber, M.; Studniarek, M.; Doh, W.H.; Zafeiratos, S.; Joly, L.; Sirotti, F.; Silly, M.G.; Gaspar, A.B.; Real, J.A.; et al. Hysteresis and change of transition temperature in thin films of  $\text{Fe}\{[\text{Me}_2\text{Pyrz}]_3\text{BH}\}_2$ , a new sublimable spin-crossover molecule. *J. Chem. Phys.* **2015**, *142*, 194702. [[CrossRef](#)] [[PubMed](#)]
37. Madeja, K. Darstellung und magnetisches Verhalten von  $[\text{Fe}(\text{phen})_2\text{X}_2]$ -Komplexen. *Chemické Zvesti* **1965**, *19*, 186–191.
38. Baker, W.A., Jr.; Bobonich, H.M. Magnetic Properties of Some High-Spin Complexes of Iron(II). *Inorg. Chem.* **1964**, *3*, 1184–1188. [[CrossRef](#)]
39. Blundell, S. *Magnetism in Condensed Matter*; Oxford University Press Inc.: New York, NY, USA, 2001.
40. Lee, J.-J.; Sheu, H.; Lee, C.-R.; Chen, J.-M.; Lee, J.-F.; Wang, C.-C.; Huang, C.-H.; Wang, Y. X-ray Absorption Spectroscopic Studies on Light-Induced Excited Spin State Trapping of an Fe(II) Complex. *J. Am. Chem. Soc.* **2000**, *122*, 5742–5747. [[CrossRef](#)]



© 2018 by the authors. Licensee MDPI, Basel, Switzerland. This article is an open access article distributed under the terms and conditions of the Creative Commons Attribution (CC BY) license (<http://creativecommons.org/licenses/by/4.0/>).